

DEFORMATION MONITORING OF A SLOPE BY VISION METROLOGY

S. Miura^{a,*}, S. Hattori^b, K. Akimoto^c, S. Nishiyama^d

^a Kajima Technical Research Institute, 2-1-1 Tobitakyu, Chofu-shi, Tokyo, Japan - miuras@kajima.com

^b Faculty of Eng., Fukuyama University, Gakuencho 1, Fukuyama-shi, Hiroshima, Japan - hattori@fui.fukuyama-u.ac.jp

^c Shikoku Polytechnic College, Gunge-cho3202, Marugame-shi, Kagawa, Japan - akimoto@shikoku-pc.ac.jp

^d Faculty of Eng., Kyoto University, Yoshidahoncho, Sakyo, Kyoto, Japan - nishiyama@geotech.kuciv.kyoto-u.ac.jp

Commission PS WG V/1

KEY WORDS: Photogrammetry, Statistics, Design, Measurement, Monitoring, Simulation, Experiment, Three-dimensional

ABSTRACT:

This paper discusses monitoring of slope deformations by vision metrology with a CCD camera. Reflective targets are placed over a slope, and their object coordinates are measured by a photogrammetric technique. Precision and sensitivity of slope deformation measurement using vision metrology are investigated. Deformation of targets placed on a slope was detected by measurement at two time epochs using hypothesis testing, and a series of equations is derived for the detection. The strengths of the observation networks were evaluated from three view points, i.e. precision of target object coordinates, sensitivity of observations and reliability of observation. Model experiments were carried out to verify the method's validity. A slope model of 1.1 m × 0.5 m in size was constructed. An reasonable exposure configuration is looked for, which is capable of detecting displacement of about 2 mm per 30 m. It is thus clarified that sufficient precision, sensitivity and reliability are achievable for practical use by a total of 12 exposures: four for each of three locations.

1. INTRODUCTION

It is important to carry out periodic observations of slope deformations, both for disaster prevention during construction and for maintenance / management. Methods for detecting slope deformation include measurement of object coordinates of targets placed in danger locations using GPS observation networks, measurement with observation networks of high precision total station, and installation of strain sensors such as optical fibers. However, these methods have not been widely employed due to their long measurement time and/or high cost. This study proposes a method for measuring displacements with vision metrology using a digital camera (Fraser, 1984; Fraser, 1985).

In general it is hard to keep an ideal observation configuration for in-situ slope measurement, unlike for industrial measurements. Network design seeks observation conditions that can give satisfactory measurement results. However, it is difficult to obtain an analytical solution. An observation configuration is often pre-determined by geographical observation constraints and prior knowledge of displacements. In this study a deformed location is assumed to be predictable in advance. And our purpose is to obtain an appropriate observation configuration to detect whether deformation has occurred on the slope. From practical point of view, it is not assumed that any absolute control points are available, but assumed that a few of fixed points exist.

2. DEFORMATION OBSERVATION MODELS AND DETECTION CAPABILITY CRITERIA

Figure 1 shows a typical model of a slope and camera configuration. The X, Y and Z axes are defined as horizontal, vertical and up-dipping directions against the sloping plane. Assuming that an unstable part of the slope is known, an environment for detecting whether Block B moved against the upper A region was considered. In reality, there are many sites that are continuously monitored to determine whether or not existing cracks have extended. It should be natural to place the targets in grid pattern both side of the boundary line as shown in Figure 1. Because there is a limited number of photo taking positions on the road slope, it is assumed that a photo is taken from below the road looking up.

In general, the following four points were taken into account in the deformation detection (Kiamehr, 2003; Benzao, 1995).

- (1) Observation precision – This refers to the internal precision obtained from a variance-covariance matrix for the space coordinates. The space coordinates need to satisfy the given precision requirements.
- (2) Deformation detection sensitivity – When object coordinates are measured with two epochs of time, the probability of first order and second order errors needs to be sufficiently low for the lower limit of the deformation to be detected.
- (3) Gross error detection reliability – When gross errors are included, observation networks need have enough redundancy to be able to detect and delete them. Well known detection methods include the data snooping method, the balanced least square method and the robust estimate method (Koch, 1999a).
- (4) Observation cost – Although it is important, it is difficult to formulate so it is not taken into account.

* Corresponding author.

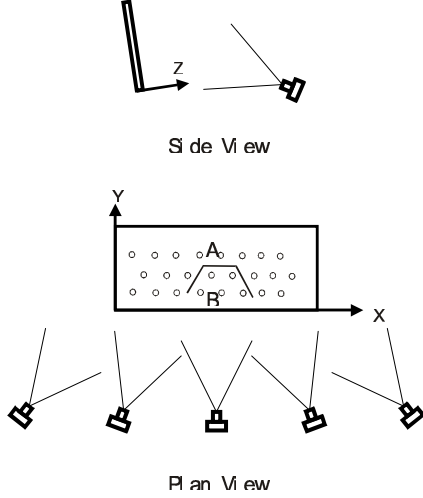


Figure 1. Model of slope and exposure configuration

3. PRECISION OF TARGET COORDINATES

Target number and object coordinates are expressed as $P_1(X_1, Y_1, Z_1), P_2(X_2, Y_2, Z_2), \dots$. Observation equations of bundle adjustment for the vision metrology at the two epochs of time (hereinafter expressed by suffix I and II) are shown below.

$$v = A_1 x + A_2 X + e : P \quad (1)$$

where v is error vector; A_1 and A_2 are design matrices for size (m, q) and (m, n) ; x is the vector for internal and external orientation, respectively; X is the space vector of the target; e is a discrepancy vector; and P is a weight matrix. This gives the weight of the observation for the image coordinate with unit. Observed values of image coordinates are assumed to be independent.

By applying the least square method to Equation (1), and eliminating x , and equivalent observation equations are obtained as follows:

$$V = A_2 X + e : P_\lambda \quad (1')$$

$$P_\lambda = P - P A_1 (A_1^T P A_1)^{-1} A_1^T P$$

Because there are no absolute datum points, the rank of the observation equations decreases by 7. Thus, constraints are added so that the mean variance of the space coordinates becomes a minimum. The most probable value of space coordinates of the targets \hat{X} and variance-covariance matrix $\Sigma_{\hat{X}}$ are given as:

$$\left. \begin{aligned} \hat{X} &= -Q^+ A_2^T P_\lambda e \\ \Sigma_{\hat{X}} &= \hat{\sigma}_0^2 Q^+ \\ \hat{\sigma}_0^2 &= \hat{V}^T P_\lambda \hat{V} / f, \quad f = m - n + 7 \\ Q &= A_2^T P_\lambda A_2 \end{aligned} \right\} \quad (2)$$

where $\hat{\sigma}_0^2$ is an observation variance of the unit weight. $\hat{\sigma}_0^2$ is a posteriori estimate. The most probable value of object space coordinates should be at least smaller than the deformation criterion to be detected.

4. SENSITIVITY OF DEFORMATION MEASUREMENT

This paper adopts the simultaneous adjustment of object space coordinates of targets for epoch I and epoch II. Another alternative is to compare the coordinates of the targets by superposing the coordinates after independently adjusting the observations (Benzao). Because different cameras were used for the two epochs, internal orientation elements were set to be independent for each epoch. The targets in Block A were common for the two epochs. The targets in Block B are treated to different for each epoch and were tagged differently. X denotes the common target coordinates, while X_I and X_{II} denote the target coordinates numbered as different targets. The equation of the adjustment calculation is as follows:

$$v = [A_{1I} \ A_{1II}] \begin{bmatrix} X_I \\ X_{II} \end{bmatrix} + A_2 \begin{bmatrix} X \\ X_I \\ X_{II} \end{bmatrix} + e : P \quad (3)$$

A variance covariance matrix $\Sigma_{\hat{Y}}$ of $Y = [X^T \ X_I^T \ X_{II}^T]^T$ is obtained in the same way as Equation (2) as follows:

$$\Sigma_{\hat{Y}} = \begin{bmatrix} \Sigma & * & * \\ * & \Sigma_I & \Sigma_{I,II} \\ * & \Sigma_{II,I} & \Sigma_{II} \end{bmatrix} \quad (4)$$

To detect the deformation, the coordinate difference d is tested.

$$d = \hat{X}_I - \hat{X}_{II} \quad (5)$$

The variance covariance matrix Σ_d for d is obtained as follows:

$$\Sigma_d = \Sigma_I - \Sigma_{I,II} - \Sigma_{II,I} + \Sigma_{II} \quad (6)$$

The relationship between the displacement vector d and the parameter used for the testing C is given by:

$$V_M + M C = d \quad (7)$$

If the number of points included in Block B is p and they have common deformation property, M becomes a matrix of $3p \times 3$ derived by gathering the p unit matrices.

$$M = [E \ E \dots \ E]^T \quad (8)$$

A weight matrix P_M is:

$$P_M = \sigma_0^2 \Sigma_d^{-1} \quad (9)$$

The most probable value of C and its variance – covariance matrix are:

$$\hat{c} = (M^T P_M M)^{-1} M^T P_M d \quad (10)$$

$$\left. \begin{aligned} \Sigma_c &= \sigma_0^2 Q_c^{-1} \\ Q_c &= M^T P_M M \end{aligned} \right\} \quad (11)$$

σ_0^2 is a priori variance factor of unit weight obtained from Equation (1) or Equation (3). Since the number of targets in Block B should be small, the posteriori variance obtained from Equation (7) is not employed.

To evaluate whether Block B was deformed, the null hypothesis

$$H_0 : c = 0 \quad (\text{No deformation occurring})$$

is tested against the alternative hypothesis

$$H_a : c = \hat{c} \neq 0 \quad (\text{Deformation occurring})$$

Assuming that the null hypothesis is correct, the tested statistical quantity is given with unknown σ_0^2 by:

$$T = \hat{c}^T Q_c^{-1} \hat{c} / (r \hat{\sigma}_0^2) \sim F(r_c, f_I + f_{II}) \quad (12)$$

where f_I and f_{II} are f in Equation (2) for respective epochs or degrees of freedom of observations, and $r_c = \text{rank}(Q_c)$ and $F(r, f)$ means F-distribution with degree of freedom (r, f) .

if a value of T is larger than a value T_α at the level of significance α , the null hypothesis can be rejected.

Secondly testing power is considered. If the alternative hypothesis is correct, the tested statistics with unknown variance factor σ_0^2 becomes:

$$T = \hat{c}^T Q_c^{-1} \hat{c} / (r \hat{\sigma}_0^2) \sim F'(r, f_I + f_{II}, \delta^2) \quad (13)$$

where F' is non-central F -distribution, and δ^2 is a non-centrality and is expressed as:

$$\delta^2 = \hat{c}^T Q_c^{-1} \hat{c} / \sigma_0^2 \quad (14)$$

Because σ_0^2 is unknown, it is replaced by a priori variance. A non-centrality δ_0^2 is determined so that the second kind error probability at T_α equals $1 - \beta$ for the given β . Then, it is sufficient if the following is valid for every target.

$$\delta^2 > \delta_0^2 \quad (15)$$

5. RELIABILITY OF NETWORKS CAPABLE OF DETECTING GROSS ERROR

The data snooping method tests whether there exists gross errors in the observations for Equation (1) in the object

coordinates that the epoch of each time is tested with. The symbol of epoch is omitted in the following equations. It is not impossible to assume that there are multiple gross errors in a single set of observations. However, here it is assumed that at most one gross error exists in the observations. The following null hypothesis

$$H_0 : E(e | H_0) = A_2 X \quad (16)$$

is tested against the following alternative hypothesis.

$$H_a : E(e | H_a) = A_2 X + Z_k \nabla s \quad (17)$$

where ∇s is magnitude of a gross error and a scalar. Z_k is a $(m, 1)$ vector and denotes the location of the gross error. The k -th element is set to 1 and the others to 0, if testing that there is a gross error in the k -th ($k = 1, \dots, m$) observation.

With the unknown variance of unit weight σ_0^2 , the following series of equations hold for the alternative hypothesis (Koch, 1999b).

By specifying $\text{rank}(A_2) = r_A = n - 7$.

$$\left. \begin{aligned} T &= \{R/1\} / \{\Omega_1 / (m - r_A - 1)\} \\ &\sim F'(1, m - r_A - 1, \delta^2) \\ \delta^2 &= \nabla \hat{s}^T Q_s^{-1} \nabla \hat{s} / \sigma_0^2 \\ \Omega &= \hat{V}^T P_\lambda \hat{V} = e^T P_\lambda Q_{\hat{V}} P_\lambda e \\ \Omega_1 &= \Omega - R \\ R &= \nabla \hat{s}^T Q_s^{-1} \nabla \hat{s} = \hat{V}^T P_\lambda Z_k Q_s Z_k^T P_\lambda \hat{V} \\ \nabla \hat{s} &= Q_s Z_k^T P_\lambda Q_{\hat{V}} P_\lambda e = -Q_s Z_k^T P_\lambda \hat{V} \\ Q_s &= (Z_k^T P_\lambda Q_{\hat{V}} P_\lambda Z_k)^{-1} \\ \hat{V} &= -Q_{\hat{V}} P_\lambda e \\ Q_{\hat{V}} &= P_\lambda^{-1} - A_2 (A_2^T P_\lambda A_2)^{-1} A_2^T \end{aligned} \right\} \quad (18)$$

where $\nabla \hat{s}$ is the most probable value of ∇s , $Q_{\hat{V}}$ is a co-factor matrix of residuals, and Ω is a sum of a square of discrepancies when there is no gross error, R is the sum of a square of discrepancies accounted for by a gross error when there is a gross error. Ω_1 decreases, if there is a gross error, and hence T increases, then the hypothesis is rejected (it is interpreted that there was a gross error.)

The lower limit of non-centrality δ_0^2 that satisfies the testing power β for a level of significance α is evaluated for a gross error to be detected. After examining the network reliability against the individual observation j ($j = 1, \dots, m$), it is judged sufficient if the following is valid.

$$\delta^2 > \delta_0^2 \quad (19)$$

6. EXPERIMENTS

6.1 Experimental environment

To examine (1) precision, (2) sensitivity and (3) reliability for a typical slope measurement, a slope model of 1,100mm wide and 500m high was made. This was about 1/30 scale of a typical construction site of a slope along a highway. Figure 2 shows one of images exposed in the following experiment displayed on the authors' measurement system named "SUBARU".

A total of 34 targets of 5 mm in diameter were placed at 200mm intervals. This interval is a standard one between anchor bolts on road and tunnel slopes. Three points are placed on a board at the central part, displacement of which is controllable. The other 31 points were stationary. A fixture in the right centre is a special device for automatic orientation (Hattori 2002).

It is usually sufficient if a 2 mm displacement is detected over a 30 m in width. Thus, the object coordinate precision of 0.050mm is envisaged to be at least necessary as practical to satisfy the other criteria. The experiments were conducted for the case of no displacements and for the case where the board was shifted by 0.050mm in the Y direction (downward in Figure 3). The camera used was a Nikon D100 (3K × 2K pixels) with a 20 mm lens. A total of 20 images were taken. Four were taken at each of five stations at a distance of 1,000 mm, as shown in Figure 1. The four images were taken by rotating the camera by 90 degrees around the optical axis. This set of images is called Set 20. The set without displacements is called Set 20_00, while one with displacements is called Set 20_50. Similarly the set of 12 images taken at three stations, i.e. left, center and right is called Set 12. And the set of eight images exposed at two stations, i.e. left and right is called Set 8. Magnitude of the displacement is denoted by _00 and _50 in the same way. There were no differences in lighting or other physical conditions in these sets.

The most probable values of interior orientation parameters and their variance-covariance matrices used through experiments are values obtained for simultaneous adjustment of Set 20_00 and Set 20_50.

6.2 Precision of coordinate measurements

The precision (standard deviation) obtained from the adjustment calculations for Sets 20_00, 12_00 and 8_00 are shown in Table 1. The increasing tendency of standard deviation almost satisfies the error propagation law. The standard deviation for the image coordinates of the targets was about 0.0003 mm. However, an empirical value would be about 0.0005 mm even under good photo-taking conditions such as exposure, etc., based on the authors' experiences. Thus, it is thought difficult to achieve higher precision from the actual measurements. Furthermore, an ideal value obtained from the self-calibration was used for the prior calibration value of the Camera's internal orientation element. Thus, the results shown below should be discounted and regarded to be about two to three times higher. However, even so, Set 8 would ensure 1 mm precision at real scale.



Figure 2. Model a slope displayed on a screen of the measurement system "SUBARU"

Table 1. Measurement precision of object coordinates for three exposure configurations

	Set 20_00	Set12_00	Set 8_00
X (mm)	0.0050	0.0006	0.0078
Y (mm)	0.0048	0.0058	0.0072
Z (mm)	0.0148	0.0163	0.0179
Average (mm)	0.0095	0.0106	0.0120

Table 2. Measurement movement of the three points (Set20_00 and Set20_50)

	101	102	103
X (mm)	-0.0054	-0.0080	-0.0019
Y (mm)	0.0340	0.0438	0.0353
Z (mm)	0.0042	0.0053	0.0127

Table 3. F-test for displacement monitoring (Set 8_00- Set 8_50)

	T	$T_{\alpha}(95\%)$	δ_0	δ for $T'_{\beta}(20\%)$
101	8.93	2.61	2.29	3.3
101,102	10.08	2.10	3.18	3.7
101,102,103	6.04	1.89	2.45	4.0

(Set 12_00- Set 12_50)

	T	$T_{\alpha}(95\%)$	δ_0	δ for $T'_{\beta}(20\%)$
101	8.93	2.61	2.99	3.3
101,102	10.08	2.10	3.18	3.7
101,102,103	9.54	1.89	3.09	4.0

(Set 20_00- Set 20_50)

	T	$T_{\alpha}(95\%)$	δ_0	δ for $T'_{\beta}(20\%)$
101	13.1	2.61	3.62	3.3
101,102	16.4	2.10	4.05	3.7
101,102,103	14.7	1.89	3.84	4.0

6.3 Sensitivity of deformation detection

Set 20, 12 and Set 8 were examined to check whether or not 0.050 mm displacement could be detected. Table 2 shows the measured movement of the three points, i.e. Points 101, 102 and 103, in Block B obtained in the test to check whether the three points moved for Sets 20_00 and 20_50. Because there are no absolute datum points, the scale of these figures is approximate. The three points include not only parallel displacement but also rotational displacement.

F value of Equation (12) was obtained to check whether or not the three Points 101, 102 and 103 had moved. The results are shown in Table 3. F was calculated for the case where only Point 101 was tested and for the cases where two points and three points were tested. Testing capability decreased due to the rotational movement of the three points. Table 3 shows F value $T\alpha$ (95%) at $\alpha = 5\%$, square root of non-centrality δ_0 , and square root of non-centrality δ that gives $\beta = 80\%$ at $\alpha = 5\%$.

The following are found from Table 3.

- Sensitivity decreased when three points were used, because there were rotational components. It is better in practice use to avoid assuming rigid body displacement of multiple points. Thus, testing should be conducted for each point..
- If the testing capability of $\beta = 20\%$ is required, observations of three points are necessary for Set 12.
- Even if testing capability is reduced, the same number of observations as Set 12 is necessary for testing each point.
- When three points are usable, there is sufficient sensitivity for Set 8.

6.4 Detection of gross errors

Results of F testing by the data snooping for Set 20_00 are shown in Figure 3. One gross error is detected. An image of the gross error is shown in Figure 4. The point where $\alpha = 5\%$ for $F(1, m - r_A - 1)$ had about $T\alpha(5\%) = 4$, so the T value of the detected gross error is sufficiently large.

The distribution of the square root of non-centrality is investigated for Set 20_00, Set 12_00 and Set 8_00, assuming that a standard deviation of image coordinates three times as large as a priori value with unit weight, $0.0005 \times 3 = 0.0015\text{mm}$ is provided to discrepancies. Figure 5 shows an example of Set 12_00. Although the non-centrality slightly increases at both ends of the model, the mean, minimum and maximum figures are shown in Table 4. The effect of variations of camera configuration to the non-centrality is slow to react. A square root of non-centrality δ^2 for $\beta = 20\%$ at the point where $\alpha = 5\%$, is about 2.8. This is less than all values of every Set, so a sufficiently reliability is confirmed in any three sets.

Table 4. The square root of non-central values (δ) for three exposure configurations

Set	Mean	Minimum	Maximum
Set 20_00	3.27	3.12	3.66
Set 12_00	3.36	3.17	3.78
Set 8_00	3.50	3.25	3.96

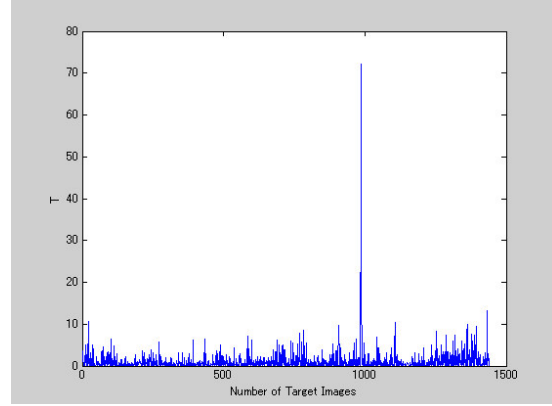


Figure 3. Results of F testing for Set 20_00

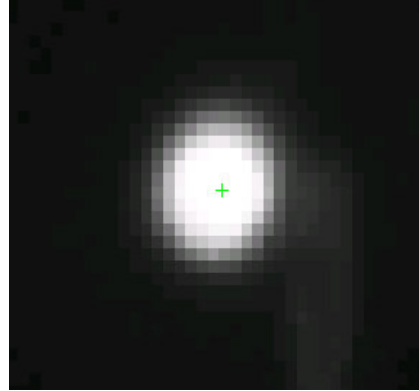


Figure 4. Image of target with gross error (Center of target is slightly deviated)

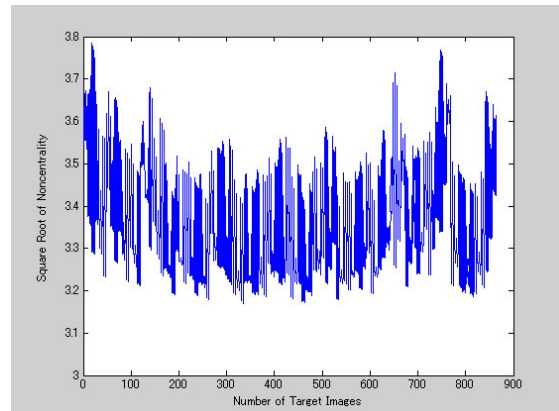


Figure 5. Distribution of square root of non-centrality; Distribution of non-centrality δ when the square root of pre-variance of error $\sigma \times 3 = 0.0015\text{mm}$ is set to every observed values for Set 12_00.

7. CONCLUSIONS AND FUTURE ISSUES TO BE TACKLED

This paper showed a procedure for detecting the displacement of slopes with vision metrology using a single digital camera. Assuming that targets were placed on the head of lock bolts applied to a slope along a typical highway with standard interval 600mm, an appropriate camera configuration, where 2 mm displacement could be detected in 30m length, was investigated. As a result, a total of 12 images or four images taken at each of three locations were shown to be clear the requirements in terms of measurement precision, sensitivity of displacement detection and reliability.

8. REFERENCES

Fraser,C.S.: Network Design Considerations for Non-Topographic Photogrammetry, *PE&RS*, Vol.50, No.8, 1984, pp.1115-1126

Fraser, C.S. and Gruendig, N.: The Analysis of Photogrammetric Deformation Measurements on Turtle Mountain, *PE&RS*, Vol.51, No.2, pp.207-216, 1985 .

Kiamehr, R.; Multi object optimization of geodetic Network, *NCC Geomatics 82 conferences*, Tehran, Iran, 2003

Benzao,T. and Z.Shaorong; Optical Design of Monitoring Networks with Prior Deformation Information, *Survey Review*, pp.33-258, 1995

Koch, K.L.: Parameter Estimation and Hypothesis Testing in Linear Models, *Springer*, pp.302-309, Berlin, 1999a

Koch, K.L.: Parameter Estimation and Hypothesis Testing in Linear Models, *Springer*, pp.279-282, Berlin, 1999b

Hattori,S., K.Akimoto, C.Fraser and H.Imoto: Automated Procedures with Coded Targets in Industrial Vision Metrology, *Photogrammetric Engineering and Remote Sensing*, Vol.68,No.5,pp.441-446, 2002